Article

pubs.acs.org/Biomac

Probing the Effects of Lipid Substitution on Polycation Mediated DNA Aggregation: A Molecular Dynamics Simulations Study

Chongbo Sun,[†] Tian Tang,*[,†] and Hasan Uludağ[‡,¶,§]

[†]Department of Mechanical Engineering, [‡]Department of Chemical and Materials Engineering, [¶]Department of Biomedical Engineering, and [§]Faculty of Pharmacy and Pharmaceutical Sciences, University of Alberta, Edmonton, Canada

Supporting Information

ABSTRACT: Understanding the molecular mechanism of DNA aggregation and condensation is of importance to DNA packaging in cells, and applications of gene delivery therapy. Modifying polycations such as polyethylenimine with lipid substitution was found to improve the performance of polycationic gene carriers. However, the role of the lipid substitution in DNA binding and aggregation is not clear and remains to be probed at the molecular level. In this work, we elucidated the role of lipid substitution through a series of all-atom molecular dynamics simulations on DNA aggregation mediated by lipid modified polyethylenimine (lmPEI). We found that the lipids associate significantly with one another, which links the lmPEIs and serves as a mechanism of aggregating the DNAs and stabilizing the formed polyplex. In addition, some lipid tails on the lmPEIs stay at the periphery of the lmPEI/DNA polyplex and may provide a mechanism for hydrophobic interactions. The enhanced stability and hydrophobicity might contribute to better cellular uptake of the polyplexes.

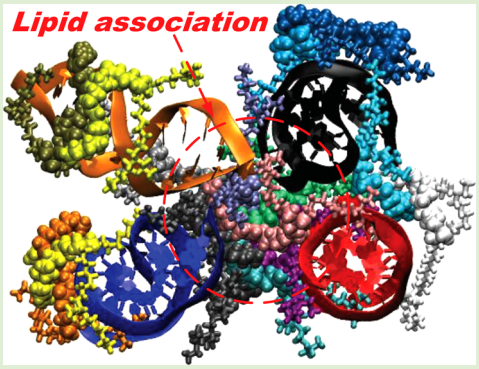

1. INTRODUCTION

Gene delivery has been extensively studied in the past two decades as a means to treat diseases associated with defective gene expression.[1,2] Although there have been as many as 1786 clinical trials to date,[3] the lack of safe and efficient gene delivery carriers is still a major impediment for the successful application of such treatment. Polycations, such as polyethylenimine (PEI),[4,5] are an important category of nonviral carriers since they are effective and do not arouse the safety concerns associated with viral carriers.[6,7] Moreover, compared with viral carriers, polycationic carriers have the advantage of being readily engineered with other functional groups, making it possible to tailor their properties for different applications. Experimentally, it has been found that modifying polycations with lipophilic and hydrophobic moieties can enhance the performance of polycation-based gene delivery carriers.[8] Khalil et al.[9] and Pham et al.[10] investigated the cellular interaction and transfection efficiency of lipid modified peptides, and found that the lipid modification yielded more stable polyplexes and led to higher cellular uptake. Hydrophobic modification of chitosan was also found to facilitate DNA condensation by forming stable polyplexes with DNA and to enhance gene delivery with improved cell entry.[11−13] Lipid modification of poly-L-lysine was found to greatly enhance the DNA delivery efficiency due to increased cellular uptake and better protection from DNA degradation.[14−17] Neamnark et al. studied the delivery and transfection efficiency of 2 kDa PEIs modified with caprylic, myristic, palmitic, stearic, oleic and linoleic acids.[18] They found that as little as one lipid substitution per PEI (with linoleic acid substituent) could transform the ineffective 2 kDa native PEI into effective carriers comparable with highly effective 25 kDa PEI. Bahadur et al. investigated the efficiency of 0.6, 1.2, and 2 kDa PEIs modified by palmitic acid, and found that the lipid substitution led to a higher zeta potential of the formed polyplexes, increased cell uptake of the DNA, and enhanced transgene expression.[19] Despite the experimental evidence, the molecular mechanism contributing to the beneficial effects of such modification in gene delivery is not clear, and remains to be investigated.

Two recent works have attempted to address the effect of lipids on the aggregation of DNA. Patel and Anchordoquy experimentally investigated the spermine and lipospermine induced DNA condensation.[20] They found that while lipospermines gave higher DNA binding affinity due to their higher hydrophobicity, they lacked the capacity to condense the DNA into compact toroidal structures. The steric hindrance introduced by the acyl chain in lipospermine was postulated to preclude packaging of DNA into compact dimensions. Posocco et al., using mesoscopic coarse-grained simulations, studied the binding of cholesterol-modified dendrimers to DNAs.[21] It was shown that the cholesterol modified dendrimers could form self-assembly through the interaction among the hydrophobic units (cholesterol), which was a reason they could condense DNA more effectively compared with native dendrimers. The influence of lipids on peptide aggregation was investigated in

Received: July 6, 2012
Published: August 1, 2012

the recent work by Hung et al.[22] and Todorova et al.[23] via computer simulations. They found that in the absence of lipids, peptides manifested higher flexibility and aggregated through interactions among the aromatic cores. In the presence of lipids, the head lipid groups more favorably interacted with the hydrophilic regions on the peptides while the lipid tails mainly interacted with the hydrophobic regions. Such interactions interfered with the interactions among the aromatic cores and prohibited the aggregation of peptides. Clearly, lipids can have different roles that may contribute positively or negatively to the aggregation; this demands a careful examination on DNA aggregation mediated by lipid modified polycations.

Computer simulations, especially all-atom molecular dynamics (MD) simulations, have proven to a powerful tool in studying interaction of polycations with nucleic acids, viruses and other drug molecules.[24−35] For example, besides the works mentioned above, all-atom MD simulations has been used to evaluate the ability of different copolymers to incorporate lipophilic drugs into micelles, which yielded results in good comparison with experimental data.[35] In this work, in order to elucidate the role of lipid substitution in polycation mediated DNA aggregation and condensation, we performed a series of large scale all-atom MD simulations. PEI was considered as the representative polycation and oleic acid (C18, 1) as the representative lipid substituent in this study. Our study determined the location of the lipid moieties in the formed polyplexes, and shed light on the effects of lipid substitution on DNA binding and aggregation.

2. METHODS

2.1. Simulated Systems and Procedure. The DNA simulated in this work was a Drew-Dickerson dodecamer $d(CGCGAATTCGCG)_2$ carrying a total charge of −22. The initial structure of the DNA was built to be a canonical B form using AMBER NAB tool.[36] The lmPEI simulated is a 831 Da branched PEI consisting of 13 amine groups with a single oleic acid (OA) lipid tail grafted on a primary amine. The chemical structure and protonation sites of the lmPEI are shown in Figure 1. A total of six primary or secondary amines were chosen to be

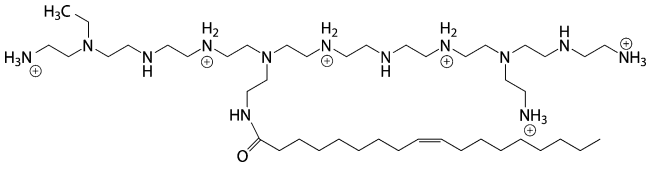

Figure 1. Molecular structures and protonation sites of the lipid modified PEI studied in this work.

protonated corresponding to a protonation ratio of 46%. We chose the 46% protonation ratio to be consistent with the protonation ratio of 47% for 600 Da PEI at pH = 6 from our recent study.[37] The protonation sites were distributed as uniformly as possible to minimize thermodynamic interactions between the protonated amines.[32] The initial structure of the lmPEI was built in VMD[38] and then energetically minimized in NAMD.[39] Five separate systems were simulated in this study, and their information is summarized in Table 1. To get an equilibrated configuration of the lmPEI, system lmPEI consisting of a single lmPEI molecule with explicit water and counterions was first simulated for 6 ns. The configuration of the lmPEI at the end of the simulation was adopted as the initial configuration of the lmPEIs in the following simulations. To study the interaction of one DNA with one lmPEI, and to determine the location of the cationic and lipophilic moieties of the lmPEI relative to the DNA, system 1D-1P containing one DNA and one lmPEI was simulated for 50 ns. The initial configuration of system 1D-1P is shown in Figure 2a, where the principal axes of the lmPEI were aligned

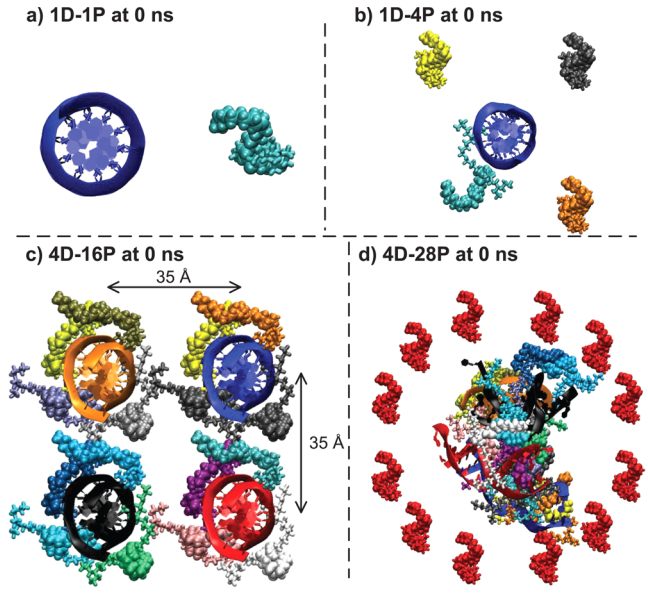

Figure 2. Snapshots of the initial configurations: (a) 1D-1P at 0 ns, (b) 1D-4P at 0 ns, (c) 4D-16P at 0 ns, (d) 4D-28P at 0 ns. Different lmPEIs are represented by different colors (except in panel d where the extra 12 lmPEIs are in red); the OA moieties on the lmPEIs are represented by spheres; water and counterions are removed for clarity.

parallel to the DNA axis and its center of mass (COM) was positioned at 25 Å from the DNA COM. To investigate the binding of multiple lmPEIs to a DNA, we adopted the final configuration of 1D-1P and added three more lmPEIs to form the new system 1D-4P. The added 3 lmPEIs in 1D-4P were again aligned parallel to the DNA axis with their COM at 25 Å away from the DNA COM (Figure 2b). The 1D-4P system was simulated for 100 ns. Four identical equilibrated 1D-4P complexes were then used to construct the system 4D-16P to study lmPEI mediated DNA aggregation. The four 1D-4P complexes were arranged on the four corners of a square, as shown in Figure 2c. The axes of the four DNAs were aligned to be parallel and the COM of each 1D-4P complex was separated from the COM of its neighboring complex by 35 Å. The 4D-16P system was simulated for 100 ns. To investigate the effect of excess lmPEIs on the DNA aggregation, 12 lmPEIs were added to the 4D-16P system at the end of the 100 ns simulation, and the new system is referred to as 4D-28P. The added 12 lmPEIs surrounded the 4D-16P polyplex in a circular fashion located at 42 Å from the COM of 4D-16P system as shown in Figure 2d. The

Table 1. Information of the Five Systems Simulated in This Study

system name	number of DNA/lmPEI	charge ratio DNA/lmPEI	no. of atoms	size of simulation box (Å^3)	no. of Na^+/Cl^-	simulation time (ns)
lmPEI	0/1	0/6	12856	64 × 48 × 41	0/6	6
1D-1P	1/1	22/6	34210	74 × 69 × 66	22/6	50
1D-4P	1/4	22/24	65285	81 × 92 × 86	0/2	100
4D-16P	4/16	88/96	96278	104 × 105 × 87	0/8	100
4D-28P	4/28	88/168	163034	117 × 117 × 117	0/80	200

dx.doi.org/10.1021/bm301045b | Biomacromolecules 2012, 13, 2982−2988

4D-28P system was simulated for 200 ns. It should be pointed out that there are many ways of specifying the initial configurations for systems 4D-16P and 4D-28P. One particular reason the present initial configurations are chosen is that the same initial configurations were used in a previous work on native PEI mediated DNA aggregation.[33] Having the same initial setting allows us to best address the influence of lipid in the DNA aggregation. To facilitate the data presentation, in systems 4D-16P and 4D-28P, each DNA is labeled with a capital letter (A, B, C, or D), and each lmPEI is labeled with a number (1−16 in 4D-16P; 17−28 for the additional 12 lmPEIs in 4D-28P).

2.2. Simulation Details. A CHARMM format force field was developed and validated[32] for PEI based on the CHARMM General Force Field,[40] and CHARMM 27 force field[41,42] was used for all other molecules. All simulations were performed using NAMD.[39] A time step of 2 fs, TIP3P water model,[43] periodic boundary condition, full electrostatics with particle-mesh Ewald method,[44] cutoff of 12 Å for van der Waals interactions and electrostatics pairwise calculations, and the SHAKE algorithm[45] were used for all the simulations. During each simulation, the system was first minimized for 5000 steps. The system was then heated from 0 to 300 K in 20 ps with 10 kcal/(mol Å^2) harmonic restraint on the non-hydrogen atoms of the DNAs and lmPEIs. The simulation was continued for 4 ns at 300 K and 1 bar with the restraint to have the ions relax around the solutes. We then removed the restraint and NPT ensemble simulation was performed for the period of time indicated in Table 1 for each system. The length of the simulations was shown to be sufficient to generate dynamic equilibrium, an evidence of which is given in Supporting Information. VMD[38] was used for visualization and trajectories analysis.

3. RESULTS AND DISCUSSION

3.1. Location of Lipophilic Moieties and Lipid Association. Although the size and charge of the carrier/DNA polyplexes are routinely assessed in an experimental setting, the structural details especially the location of the lipophilic moieties in the lipid-modified polycation/DNA polyplexes have not been investigated.[8] Figure 3 shows the final configurations for systems 1D-1P, 1D-4P, 4D-16P, and 4D-28P, where the lipid moieties on the lmPEIs are represented by spheres. In system 1D-1P (Figure 3a), the cationic moiety of the lmPEI conforms to the DNA while the lipid tail remains on the outside with no obvious interactions with the DNA molecule. In system 1D-4P (Figure 3b), the four lipid tails still stay outside of the complex with three of them being associated with one another. In system 4D-16P (Figure 3c), a DNA aggregate is formed and a large lipid association involving multiple lmPEIs is formed in the middle of the four DNA molecules. The remaining lipids also stay associated with one another on the periphery of the DNA aggregate. In system 4D-28P (Figure 3d), the DNA aggregate and the large lipid association continue to exist. In addition, some of the added lmPEIs are attached to the outer surface of the formed DNA aggregate.

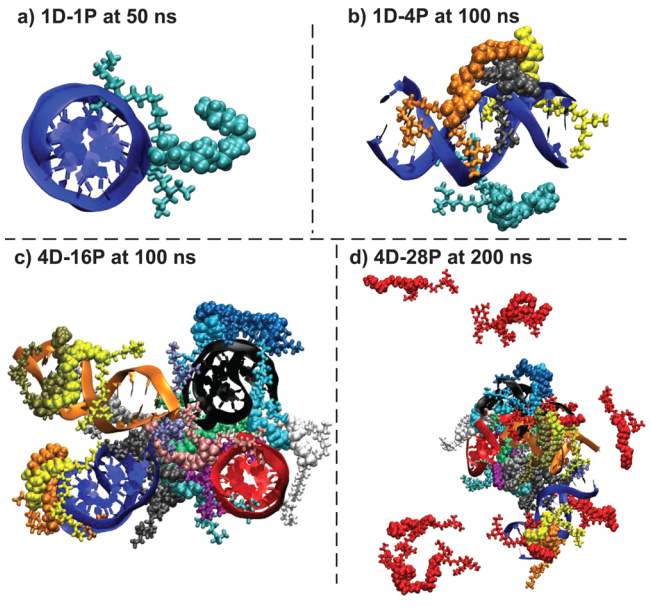

Figure 3. Snapshots of the final configurations: (a) 1D-1P at 50 ns, (b) 1D-4P at 100 ns, (c) 4D-16P at 100 ns, and (d) 4D-28P at 200 ns. Different lmPEIs are represented by different colors (except in panel d where the extra 12 lmPEIs are in red); the OA moieties on the lmPEIs are represented by spheres; water and counterions are removed for clarity.

To quantify the location of cationic and lipophilic moieties of the lmPEIs relative to the DNA, in Figure 4 we plotted the cumulative percentage of the lmPEI nitrogens and lipid carbons for system 1D-4P as a function of distance from any DNA C1′ atom, averaged over the last 40 ns of the simulation. The C1′ atoms are on the sugar rings of the DNAs, located inside the DNA helix at a distance of ∼5 Å from the surface of DNA defined by the phosphorus atoms. In Figure 4, taking the lmPEI nitrogens for example, the cumulative percentage at a given distance r is the percentage of all the lmPEI nitrogens within a distance r from any DNA C1′ atoms. The curve for the lmPEI nitrogens rises quickly from 0% at 4 Å to ∼90% at 9 Å, demonstrating that most lmPEI nitrogens stay between 4 and 9 Å from the DNA C1′ atoms. The curve for the lipid carbons only reaches ∼30% at 10 Å, indicating that only ∼30% of the lipid carbons are within 10 Å of the DNA C1′ atoms. These curves clearly show that, as observed visually in Figure 3b, the cationic moieties bind closely to the DNA while the lipid substituents tend to stay away from the DNA instead of being located inside the DNA grooves.

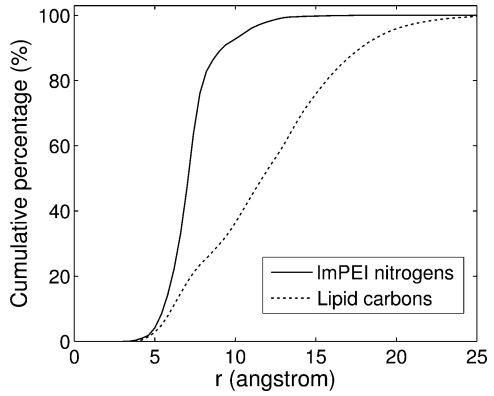

Figure 4. Cumulative percentage of the lmPEI nitrogens and lipid carbons as functions of the distance from any DNA C1′ atom in system 1D-4P.

As seen in Figure 3c, the lipid moieties that stay on the periphery of the lmPEI/DNA complex become associated with one another when multiple lmPEI/DNA complexes are placed together. This can play a significant role in aggregating the DNAs. To quantify the association among the lipid tails in the aggregate, in Figure 5 we tabulated, between each pair of lipid tails, the number of pairs of lipid carbons that are closer than 5 Å apart, averaged over the last 40 ns of the simulations. The calculations were performed for both systems 4D-16P and 4D-

dx.doi.org/10.1021/bm301045b | Biomacromolecules 2012, 13, 2982−2988

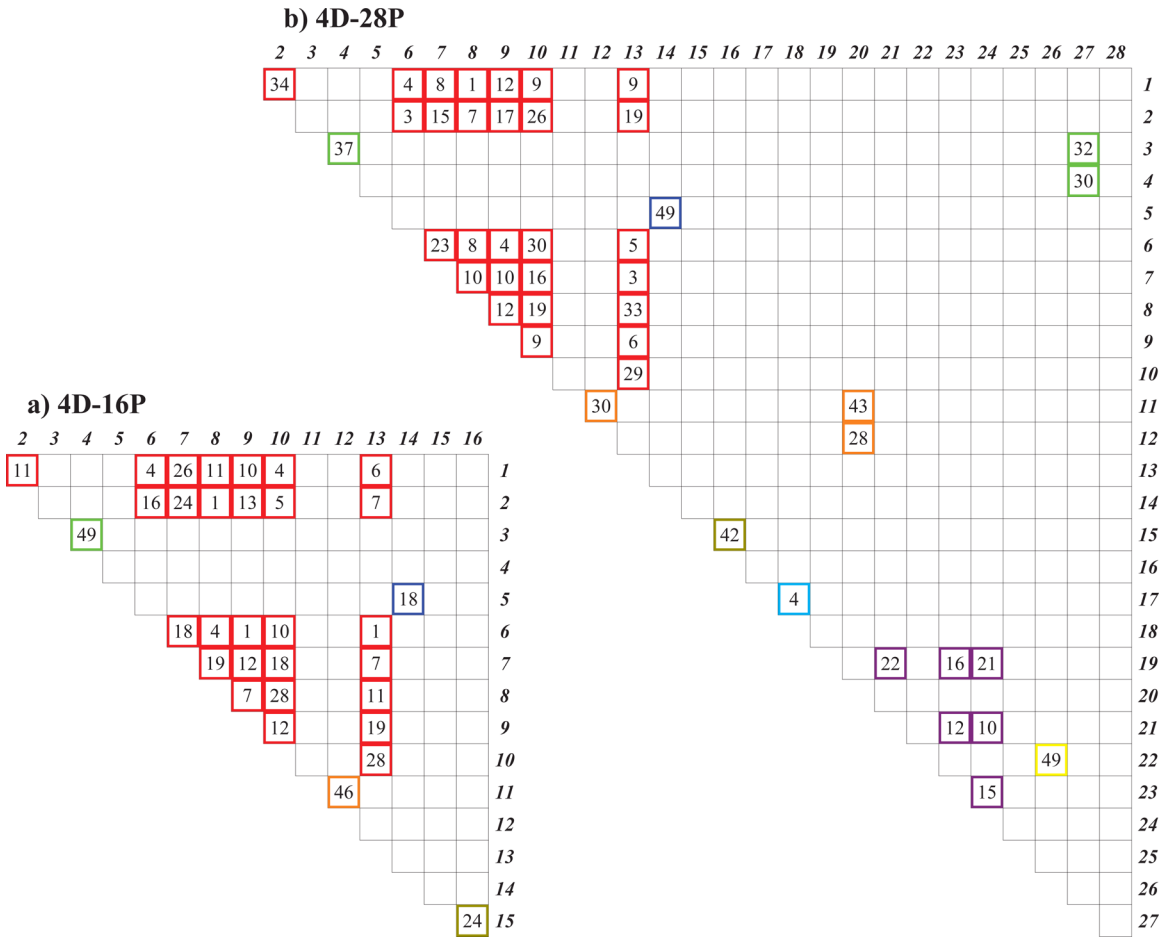

Figure 5. Number of pairs of lipid carbons that are closer than 5 Å apart between each pair of lipid tails in (a) 4D-16P, and (b) 4D-28P. The numbers on the top and right of each subfigure are lmPEI indices. Only the nonzero numbers are shown and marked with colored squares. The lmPEIs involved in the same association are marked by the same color.

28P. The numbers on the top and right of each subfigure are the lmPEI indices. Each pair of lmPEIs in a system can form a pair of lipid tails. This results in 120 pairs of lipid tails in systems 4D-16P and 378 pairs in 4D-28P, corresponding to 120 cells in Figure 5a and 378 cells in Figure 5b, respectively. Each lipid tail has 18 carbons; thus, between a pair of lipid tails there are 324 pairs of carbons. Among these 324 pairs of carbons, the number of pairs within 5 Å is counted and given in the cell corresponding to this pair of lipid tails. The cell is left empty where no carbon pairs are found to be within 5 Å. For example, number 11 on the top left cell of Figure 5a means that out of the 324 pairs of carbons between lmPEI 1 and lmPEI 2 in system 4D-16P, 11 pairs are separated by 5 Å or less. We choose 5 Å as the criterion because this is the closet carbon−carbon distance within which the free energy for the association of two alkane molecules is negative indicating that their associaltion is energetically favorable.[46] If one or more pairs of lipid carbons between two lipid tails is closer than 5 Å apart, the two lipid tails are said to be associated. In Figure 5a, consider the rows 1, 2, 6−10 and columns 2, 6, 7, 8, 9, 10, 13; all the cells formed by these rows and columns have nonzero numbers, which are marked with red squares. This indicates that lmPEIs 1, 2, 6−10, and 13 are mutually associated and they form a large association involving 8 lmPEIs in system 4D-16P. It can be seen in Figure 3c that this association stays in the middle of the polyplex. Since the 8 lmPEIs bind to different DNAs, the lipid association contributes to holding the DNAs in an aggregated form. Four other lipid associations each involving only two lmPEIs also exist in the polyplex (illustrated by the squares of green, blue, orange and olive colors in Figure 5a). Overall, each lmPEI in system 4D-16P is associated with at least one other lmPEIs through lipids, demonstrating the significance of lipid association in the polyplex.

In system 4D-28P, the 12 extra lmPEIs are indexed by numbers 17−28, as shown in Figure 5b. Comparing the columns 2−16 of Figure 5b with Figure 5a, it can be seen that all the colored squares stay in the same location. This means that, after adding 12 more lmPEIs, the lipid associations formed in system 4D-16P preserve in system 4D-28P. In addition, lmPEI 27 joins the lipid association between lmPEIs 3 and 4 (3 cells marked by green squares in Figure 5b); lmPEI 20 joins the lipid association between lmPEIs 11 and 12 (3 cells marked by orange squares in Figure 5b); lmPEIs 19, 21, 23, and 24 form a new association involving four lmPEIs (6 cells marked by violet squares in Figure 5b); lmPEIs 17 and 18 are associated (cyan square in Figure 5b); as well lmPEIs 22 and 26 are associated (yellow square in Figure 5b). Only two lmPEIs—PEIs 25 and 28—are not associated with any other lmPEIs. It should be noted that not all the extra lmPEIs are bound to the DNA aggregate. In particular, by examining the binding state of each lmPEI with the DNAs (Figure S3 in Supporting Information), we found that, during the last 40 ns of the simulation, lmPEIs

dx.doi.org/10.1021/bm301045b | *Biomacromolecules* 2012, 13, 2982−2988

17, 20, 22, and 27 directly bind to the DNAs for more than 50% of the time. lmPEIs 18 and 26 bind directly to the DNAs for short periods of time; also they attach to the polyplex through lipid association with lmPEIs 17 and 22. lmPEIs 19, 21, 23, and 24 do not bind to any DNAs and exist in an associated form in the solution. lmPEIs 25 and 28 neither bind to the DNAs nor are associated with any other lmPEIs.

3.2. Polyion Bridging and DNA Charge Neutralization.

Two main mechanisms have been identified in native PEI mediated DNA aggregation:[33] polyion bridging (i.e., a polycation binding with multiple DNA segments simultaneously; see detailed definition in Supporting Information) and DNA charge neutralization. Not surprisingly, we found that polyion bridging also plays an important role in lmPEI mediated DNA aggregation. Specially, five lmPEIs participated in bridging two or three DNAs for longer than 50% of the simulation time in both systems 4D-16P and 4D-28P (see Figures S2 and S3 in Supporting Information). However, the intensity of polyion bridging appears to be slightly weaker than that in native PEI mediated DNA aggregation, as in both the system containing 4 DNAs with 16 native PEIs and the system containing 4 DNAs with 28 native PEIs, eight PEIs participated in bridging DNAs for longer than 50% of the simulation time.[33] We attribute this to the steric disturbance on the polyion bridging arising from the lipid tails on the lmPEIs.

To investigate how lmPEIs neutralize the DNA charges and whether the lipid modification introduces any effect on the charge neutralization, we plotted the cumulative distributions, with respect to the DNA C1′ atoms, of protonated PEI nitrogens, Cl- ions, and the net charge of PEI and ions, averaged over the last 40 ns of the simulations (Figure 6). The results for lmPEIs (left column) are compared with those for native PEIs[33] (right column). In each subfigure of Figure 6, the straight dashed black line indicates the total charge all the DNAs in the system carry, and the blue solid curve is the total charge of PEI and ions within a given distance to their nearest DNA C1′ atoms. At the distance where black line and blue curve intersect, the DNA charges are 100% neutralized by the PEI and ions. At larger distances, the PEI and ions charges exceed the DNA charges, and the DNA(s) are 'overneutralized'. It can be seen that the PEIs in all the 6 systems demonstrate similar characteristics in neutralizing the DNA(s). Quantitatively, the distance at which the lmPEIs 100% neutralize the DNA(s) is shorter than the distance at which the native PEIs 100% neutralize the DNA(s). Specifically, for system 1D-4P, such distance is ∼10 Å for lmPEIs and ∼12 Å for native PEIs. For system 4D-28P, such distance is ∼8 Å for lmPEIs and ∼10 Å for native PEIs. The distance at which the 'overneutralization' maximizes is approximately the same for all the 6 systems, being ∼15 Å. However, in excess of PEIs, the degree of overneutralization is higher for lmPEIs, which can be seen by comparing the peak values of the blue solid curves in Figure 6e,f. The overneutralization of the DNAs can also be quantified using the number of PEI molecules bound to the DNAs during the simulation. Here we say a lmPEI is bound to DNA if it has one or more nitrogens within 4 Å of any DNA N/O atoms (see Supporting Information for details). Figure 7 shows this number as a function of simulation time for the system of 4D-28P with lmPEIs. On average, 19.7 lmPEIs are directly bound with the DNAs during the last 40 ns of the simulation for system 4D-28P. These 19.7 lmPEIs carry a positive charge of 118 and the DNAs carry a negative charge of −88. Besides the lmPEIs directly bound to the DNAs, there are some lmPEIs attached to the polyplex through lipid association with the lmPEIs directly bound to the DNAs. Thus, the resulting polyplex carries a positive charge higher than +30. To compare, in the system of 4 DNAs with 28 native PEIs,[33] on average 18.2 PEIs were bound to the DNAs during the last 40 ns of the simulation. Overall, our results show that the PEI's capability in neutralizing DNA is slightly enhanced by the lipid substitution.

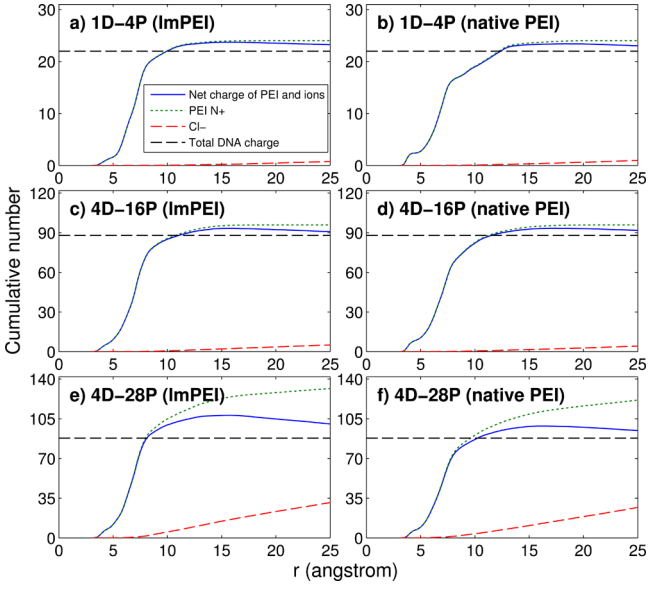

Figure 6. Cumulative numbers of PEI charges, Cl^-, and net charge of PEI/Cl^- as a function of the distance from any C1′ DNA atom (averaged over the last 40 ns of each simulation). The total charge of all the DNAs in each system is plotted by a straight dashed black lines as reference. (a) D-4P (lmPEI), (b) D-4P (native PEI), (c) 4D-16P (lmPEI), (d) 4D-16P (native PEI), (e) 4D-28P (lmPEI), (f) 4D-28P (native PEI).

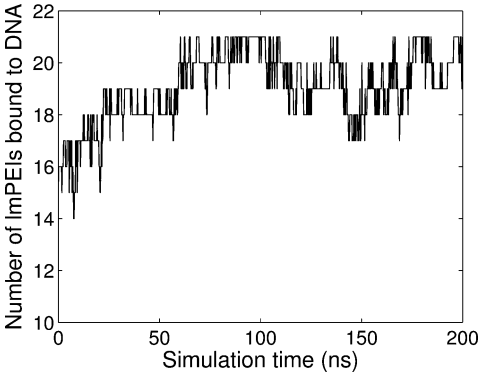

Figure 7. Number of lmPEI molecules bound to DNA during the simulation of system 4D-28P.

3.3. Water Release during the Aggregation Process.

Macromolecular association in aqueous environment is normally accompanied by the release of water molecules previously adhering to the surfaces of the macromolecules. Since the water molecules on the macromolecular surfaces are less mobile, such release is an entropically favorable process with a free energy reduction of up to 2 kcal/mol at 300 K.[47] Therefore, counting the number of water molecules released during the macromolecule association allows us to assess the

dx.doi.org/10.1021/bm301045b | Biomacromolecules 2012, 13, 2982−2988

entropic gain from water release upon macromolecular binding. Table 2 summarizes the number of water molecules released

Table 2. Number of Water Molecules Released from the Solutes during the Aggregation Process

system	4D-16P(lmPEI)	4D-16P(native PEI)	4D-28P(lmPEI)	4D-28P(native PEI)
no. of waters	1003	794	1345	844

from the hydration shell of the solutes (within 3 Å from the molecules) during the aggregation process for systems 4D-16P and 4D-28P and their counterparts involving native PEIs.[33] Detailed information on the calculation is given in Supporting Information. It can be seen that the numbers of released water molecules are much higher for the lmPEI systems than for the native PEI systems. System 4D-16P has ∼20% more water molecules released, and system 4D-28P has as high as ∼60% more water molecules released compared to its native PEI counterpart. There are two reasons for the much larger amount of water release in the presence of lmPEIs. First, there are a greater number of lmPEI molecules (>19.7) in the lmPEI/DNA polyplex than the number of native PEIs (∼18.2) in the native PEI/DNA polyplex. Second, the lmPEIs in the lmPEI/DNA polyplex are significantly associated, resulting in more water release.

3.4. Discussion. From our simulation results, several effects of the lipid substitution on DNA aggregation can be identified. First, compared with the polyplex formed by DNA and native PEIs,[33] the existence of hydrophobic moieties on the periphery of the lmPEI/DNA polyplex can present the hydrophobic groups more effectively for interaction with cell membranes and other hydrophobic biological entities on the delivery path. The external location of lipids is expected to facilitate the internalization of the DNAs through cell membranes, supporting the experimentally observed higher cellular uptake of lmPEI/DNA polyplexes compared with native PEI/DNA polyplexes.[19] The peripheral lipids can also enhance the interfacial interaction among lmPEI/DNA polyplexes and drive their growth into larger polyplexes, which is confirmed in our experimental observation that the size of lmPEI/DNA polyplex became larger after 30 min (unpublished results). Moreover, the lipids on the periphery of the polyplex can presumably reduce the accessibility of degrading nucleases to the DNA molecules and hence protect the DNAs from degradation. Second, the lmPEI/DNA polyplex formed in our simulation has demonstrated enhanced stability compared with native PEI/DNA polyplex.[33] A strong evidence of this is that when we added 12 extra PEIs to the polyplex formed by 4 DNAs and 16 native PEIs, we found that some of the original 16 PEIs were "replaced" by the added PEIs in that they unbound from the DNAs while allowing the newly added PEIs to bind to the DNAs.[33] Interestingly, this did not happen to our current 4D-28P system after adding 12 lmPEIs (see Figure S3 in Supporting Information). All the original 16 lmPEIs bound firmly to the DNAs during the entire 200 ns simulation. We attribute the increased stability to the intensive linkage formed among the lmPEIs through lipid association which we observed in systems 4D-16P and 4D-28P. In fact, despite the steric hindrance associated with the presence of the lipid tails, the radius of gyration of the four DNAs aggregated by lmPEIs is found to be nearly identical to that of the four DNAs aggregated by native PEIs (see Figure S4 in Supporting Information). The lipid association has compensated for the steric hindrance as well as the electrostatic repulsion between the likely charged lmPEIs and allowed the formation of a network in which the lmPEIs collectively aggregate the DNAs and all the DNAs are mutually connected. In contrast, native PEIs work individually in aggregating the DNAs and only a fraction of the DNAs in the aggregate are mutually connected by the native PEIs,[33] resulting in polyplexes with an overall lower stability. Another support for the enhanced stability of the lmPEI/DNA polyplex is the significantly larger amount of water molecules released from the lmPEI/DNA polyplex compared with the native PEI/DNA polyplex. Because water release is associated with entropy gain and free energy reduction, more water release contributes favorably to increase the stability of the formed polyplex. The low stability of polyplexes formed by low molecular weight (LMW) native PEIs might be a major reason for the low cellular uptake of these polyplexes. Modifying LMW PEIs with lipid substitution could overcome this drawback of native LMW PEIs while taking the advantage of the low toxicity associated with LMW PEIs. Finally, in excess of PEIs, the polyplex formed by lmPEIs and DNAs is more positively charged compared with that formed by native PEIs and DNAs. This is consistent with the experimental finding that lmPEI aggregated polyplexes have a higher ζ potential than native PEI aggregated polyplexes.[19,48]

In an experimental investigation of the dissociation of different polylexes formed by 2 kDa native PEI and 23 lmPEIs with different types and amount of lipid substitutions, it was found that 7 of the lmPEIs formed polyplexes that were more difficult to dissociate compared with native PEI formed polyplexes, while the other 16 lmPEIs formed polyplexes that were easier to dissociate.[18] This suggests that the lipid modification might weaken the stability of the polyplex in some cases. Our simulation results have shown that the degree of polyion bridging is slightly weaker for lmPEI mediated DNA aggregation. The weakened polyion bridging by lipid substitution could make the polyplex easier to dissociate while the network formed among the lmPEIs from lipid association could provide more resistance to the polyplex dissociation. For the systems studied in this work, the weakened stability from less intensive polyion bridging is more than compensated by the enhanced stability due to lipid association, and the lmPEI/DNA polyplexes manifest higher stability. However, for lmPEIs modified with different types and amount of lipid substitutions, the significance of these two effects might be reversed. The delicate balance between these two effects provides an explanation for the experimentally observed different dissociation results for lmPEIs with different lipid substitution.[18]

4. CONCLUSIONS

When lmPEIs bind with a DNA, the cationic moieties of the lmPEIs form close contact with the DNA whereas the lipid moieties stay at the periphery. Compared with native PEIs, which aggregate DNAs through polyion bridging and charge neutralization, lmPEIs mediate DNA aggregation through an additional mechanism: association among lipid tails of different lmPEIs. The lipid association is significant and it further stabilizes the lmPEI/DNA polyplex. However, the lipid substitution weakens the polyion bridging and this might have an opposite effect on the stability enhanced by lipid association. The peripheral location of the lipid moieties attached to the lmPEI/DNA polyplex increases the hydro-

phobicity of the formed polyplex and contributes favorably to the interaction of the polyplex with cell membrane.

■ ASSOCIATED CONTENT

Supporting Information

Evidence of convergence of the simulation trajectories; each PEI's binding state with the DNAs during the simulations for systems 4D-16P and 4D-28P; calculation of water release; radii of gyration of the four DNAs in systems 4D-16P and 4D-28P and comparison with their counterparts involving native PEIs; results on DNA−DNA spacing. This material is available free of charge via the Internet at http://pubs.acs.org.

■ AUTHOR INFORMATION

Corresponding Author

*E-mail: tian.tang@ualberta.ca. Phone: +1-780-492-5467. Fax: +1-780-492-2200.

Notes

The authors declare no competing financial interest.

■ ACKNOWLEDGMENTS

We acknowledge the computing resources and technical support from Compute Canada and the high performance computing facility at the National Institute for Nanotechnology, Edmonton, Canada. This work was supported by the National Science and Engineering Research Council of Canada, Alberta Innovates − Technology Futures, and Canada Foundation for Innovation.

■ REFERENCES

(1) Mulligan, R. *Science* **1993**, *260*, 926−932.
(2) Schaffert, D.; Wagner, E. *Gene Ther.* **2008**, *15*, 1131−1138.
(3) The *Journal of Gene Medicine* Clinical Trial Web Page; http://www.wiley.co.uk/genmed/clinical/.
(4) Boussif, O.; Lezoualc'h, F.; Zanta, M. A.; Mergny, M. D.; Scherman, D.; Demeneix, B.; Behr, J. P. *Proc. Natl. Acad. Sci. U.S.A.* **1995**, *92*, 7297−7301.
(5) Godbey, W.; Wu, K.; Mikos, A. *J. Controlled Release* **1999**, *60*, 149−160.
(6) Ledley, F. *Hum. Gene Ther.* **1995**, *6*, 1129−1144.
(7) Luo, D.; Saltzman, W. *Nat. Biotechnol.* **2000**, *18*, 33−37.
(8) Incani, V.; Lavasanifar, A.; Uludag, H. *Soft Matter* **2010**, *6*, 2124−2138.
(9) Khalil, I.; Futaki, S.; Niwa, M.; Baba, Y.; Kaji, N.; Kamiya, H.; Harashima, H. *Gene Ther.* **2004**, *11*, 636−644.
(10) Pham, W.; Kircher, M.; Weissleder, R.; Tung, C. *ChemBioChem* **2004**, *5*, 1148−1151.
(11) Liu, W.; Zhang, X.; Sun, S.; Sun, G.; De Yao, K.; Liang, D.; Guo, G.; Zhang, J. *Bioconjugate Chem.* **2003**, *14*, 782−789.
(12) Chae, S.; Son, S.; Lee, M.; Jang, M.; Nah, J. *J. Controlled Release* **2005**, *109*, 330−344, 12th International Symposium on Recent Advances in Drug Delivery Systems, Salt Lake City, UT, FEB 21−24, 2005.
(13) Hu, F.; Zhao, M.; Yuan, H.; You, J.; Du, Y.; Zeng, S. *Int. J. Pharm.* **2006**, *315*, 158−166.
(14) Abbasi, M.; Uludag, H.; Incani, V.; Olson, C.; Lin, X.; Clements, B. A.; Rutkowski, D.; Ghahary, A.; Weinfeld, M. *Biomacromolecules* **2007**, *8*, 1059−1063.
(15) Abbasi, M.; Uludag, H.; Incani, V.; Hsu, C. Y. M.; Jeffery, A. *Biomacromolecules* **2008**, *9*, 1618−1630.
(16) Clements, B. A.; Incani, V.; Kucharski, C.; Lavasanifar, A.; Ritchie, B.; Uludag, H. *Biomaterials* **2007**, *28*, 4693−4704.
(17) Incani, V.; Tunis, E.; Clements, B. A.; Olson, C.; Kucharski, C.; Lavasanifar, A.; Uludag, H. *J. Biomed. Mater. Res., Part A* **2007**, *81A*, 493−504.
(18) Neamnark, A.; Suwantong, O.; Bahadur, R. K. C.; Hsu, C. Y. M.; Supaphol, P.; Uludag, H. *Mol. Pharmaceutics* **2009**, *6*, 1798−1815.
(19) Bahadur, K. C. R.; Landry, B.; Aliabadi, H. M.; Lavasanifar, A.; Uludag, H. *Acta Biomater.* **2011**, *7*, 2209−2217.
(20) Patel, M.; Anchordoquy, T. *Biophys. J.* **2005**, *88*, 2089−2103.
(21) Posocco, P.; Pricl, S.; Jones, S.; Barnard, A.; Smith, D. K. *Chem. Sci.* **2010**, *1*, 393−404.
(22) Hung, A.; Yarovsky, I. *J. Mol. Graphics Modell.* **2011**, *29*, 597−607.
(23) Todorova, N.; Hung, A.; Yarovsky, I. *J. Phys. Chem. B* **2010**, *114*, 7974−7982.
(24) Ziebarth, J.; Wang, Y. *Biophys. J.* **2009**, *97*, 1971−1983.
(25) Pavan, G. M.; Danani, A.; Pricl, S.; Smith, D. K. *J. Am. Chem. Soc.* **2009**, *131*, 9686−9694.
(26) Pavan, G. M.; Kostiainen, M. A.; Danani, A. *J. Phys. Chem. B* **2010**, *114*, 5686−5693.
(27) Pavan, G. M.; Albertazzi, L.; Danani, A. *J. Phys. Chem. B* **2010**, *114*, 2667−2675.
(28) Pavan, G. M.; Mintzer, M. A.; Simanek, E. E.; Merkel, O. M.; Kissel, T.; Danani, A. *Biomacromolecules* **2010**, *11*, 721−730.
(29) Ouyang, D.; Zhang, H.; Herten, D.-P.; Parekh, H. S.; Smith, S. C. *J. Phys. Chem. B* **2010**, *114*, 9220−9230.
(30) Ouyang, D.; Zhang, H.; Parekh, H. S.; Smith, S. C. *J. Phys. Chem. B* **2010**, *114*, 9231−9237.
(31) Doni, G.; Kostiainen, M. A.; Danani, A.; Pavan, G. M. *Nano Lett.* **2011**, *11*, 723−728.
(32) Sun, C.; Tang, T.; Uludag, H.; Cuervo, J. E. *Biophys. J.* **2011**, *100*, 2754−2763.
(33) Sun, C.; Tang, T.; Uludag, H. *Biomacromolecules* **2011**, *12*, 3698−3707.
(34) Sun, C.; Tang, T.; Uludag, H. *J. Phys. Chem. B* **2012**, *116*, 2405−2413.
(35) Kasimova, A. O.; Pavan, G. M.; Danani, A.; Mondon, K.; Cristiani, A.; Scapozza, L.; Gurny, R.; Moeller, M. *J. Phys. Chem. B* **2012**, *116*, 4338−4345.
(36) Case, D.; Darden, T.; T.E. Cheatham, I.; Simmerling, C.; Wang, J.; Duke, R.; Luo, R.; Crowley, M.; Walker, R. C.; Zhang, W.; Merz, K.; B.Wang,; Hayik, S.; Roitberg, A.; Seabra, G. et al. *AMBER 10*; University of California: San Francisco, CA, 2008.
(37) Utsuno, K.; Uludag, H. *Biophys. J.* **2010**, *99*, 201−207.
(38) Humphrey, W.; Dalke, A.; Schulten, K. *J. Mol. Graphics* **1996**, *14*, 33−38.
(39) Phillips, J.; Braun, R.; Wang, W.; Gumbart, J.; Tajkhorshid, E.; Villa, E.; Chipot, C.; Skeel, R.; Kale, L.; Schulten, K. *J. Comput. Chem.* **2005**, *26*, 1781−1802.
(40) Vanommeslaeghe, K.; Hatcher, E.; Acharya, C.; Kundu, S.; Zhong, S.; Shim, J.; Darian, E.; Guvench, O.; Lopes, P.; Vorobyov, I.; MacKerell, A. D., Jr. *J. Comput. Chem.* **2010**, *31*, 671−690.
(41) Brooks, B.; Bruccoleri, R.; Olafson, D.; States, D.; Swaminathan, S.; Karplus, M. *J. Comput. Chem.* **1983**, *4*, 187−217.
(42) MacKerel Jr., A.; Brooks III, C.; Nilsson, L.; Roux, B.; Won, Y.; Karplus, M. In *CHARMM: The Energy Function and Its Parameterization with an Overview of the Program*; Schleyer, P.v. R.; et al., Eds.; The Encyclopedia of Computational Chemistry; John Wiley & Sons: Chichester, 1998; Vol. *1*; pp 271−277.
(43) Jorgensen, W. *J. Am. Chem. Soc.* **1981**, *103*, 335−340.
(44) Darden, T.; York, D.; Pedersen, L. *J. Chem. Phys.* **1993**, *98*, 10089−10092.
(45) Ryckaert, J.; Ciccotti, G.; Berendsen, H. *J. Comput. Phys.* **1977**, *23*, 327−341.
(46) Thomas, A. S.; Elcock, A. H. *J. Phys. Chem. Lett.* **2011**, *2*, 19−24.
(47) Dunitz, J. *Science* **1994**, *264*, 670.
(48) Aliabadi, H. M.; Landry, B.; Bahadur, R. K.; Neamnark, A.; Suwantong, O.; Uludag, H. *Macromol. Biosci.* **2011**, *11*, 662−672.